Submitted to ADVANCED MATERIALS

Supporting Information

for *Adv. Mater.*, DOI: 10.1002/adma. 201603276

Black Phosphorus Nanosheets as A Robust Delivery Platform for Cancer Theranostics

Wei Tao, Xianbing Zhu, Xinghua Yu, Xiaowei Zeng, Quanlan Xiao, Xudong Zhang, Xiaoyuan Ji, Xusheng Wang, Jinjun Shi, Han Zhang* and Lin Mei**

Experimental Section

1. Materials. The bulk BP was purchased from Smart-Elements (a commercial supplier) and stored in a dark Ar glovebox. PEG-NH_2, FITC-PEG-NH_2 and FA-PEG-NH_2 were purchased from Nanocs Inc. (New York, USA). The molecular weight (MW) of PEG applied in this study is 2k Da. Cy7-NH_2 was bought from Lumiprobe Corporation (Hallandale Beach, USA). MTT and DAPI were purchased from Sigma-Aldrich (St. Louis, MO, USA). All other agents used were of the highest commercial grade available. HyPure Molecular Biology Grade Water (Hyclone^{TM}) was used to prepare all the solutions.

2. Synthesis of BP NSs. The BP NSs were prepared by a modified liquid exfoliation of corresponding bulk BP sample.[1] Briefly, 25 mg of the obtained BP was added to 50 ml of HyPure Molecular Biology Grade Water, which bubbled with argon to eliminate dissolved oxygen molecules for reducing the oxidation during the exfoliation procedure. The mixture solution was then sonicated in ice water with a sonic tip for 12 h (Amplifier: 25%, On/Off cycle: 45 s/15 s). The ice water was utilized to keep a relatively low temperature of the system. The resulting brown dispersion was centrifuged at 1000 rpm for 10 min to get rid of unexfoliated bulk BP and the supernatant containing BP NSs was carefully collected. After that, the collected supernatant with BP NSs was put into Amicon tubes (MWCO 100kDa; Millipore) and was

centrifuged at 3750 rpm (4 °C) for 30 min to get rid of the water. The obtained pure BP NSs were re-suspended in PBS or HyPure Water for further use and stored under 4 °C.

3. PEG coating on the surface of BP NSs. In order to prepare BP-PEG NSs, 10 mg of PEG-NH_2 was dispersed in 10 ml of BP NSs/H_2O solution at BP concentration of 200 μg/ml. After probe sonication for 30 min and stirring for 4 h, the resulting mixture was centrifuged in Amicon tubes (MWCO 100kDa; Millipore) at 3750 rpm (4 °C) for 30 min to remove the excess PEG molecules, and washed 2 times using the same method. The pure BP-PEG NSs sample was re-suspended in PBS or HyPure Water for further use and stored under 4 °C finally. Targeting modification BP-PEG-FA NSs or fluorescent modification BP-PEG-FITC NSs were prepared via the same technology, except FA-PEG-NH_2 or FITC-PEG-NH_2 was used instead of PEG-NH_2 and avoiding light for FITC-PEG-NH_2.

4. Preparation of PEGylated BP theranostic delivery platform. For chemotherapy DOX loading, pure BP-PEG NSs or BP-PEG-FA NSs (50 μg/ml) were mixed with different concentrations of DOX ((30, 60, 90, 120, 150, 180 or 210 μg/ml)) in PBS at pH = 7.4, and then stirred at room temperature for 24 h. The excess unloading was washed away via filtering the mixture through Amicon tubes (MWCO 100kDa; Millipore) and rinsing with HyPure water for 3 times wash. For *in vivo* NIR imaging agents Cy7-NH_2 loading, 50 μg/ml of pure BP-PEG NSs or BP-PEG-FA NSs were mixed with Cy7-NH_2 (50 μg/ml) in PBS at pH = 7.4, and then stirred at room temperature for 4 h. The excess unloading was washed away via filtering the mixture through Amicon tubes (MWCO 100kDa; Millipore) and rinsing with HyPure water for 3 times wash. The whole process was carried out avoiding light to reduce the quenching of imaging agents.

5. Characterization of PEGylated BP NSs. TEM, STEM images and EDS mapping of PEGylated BP NSs were taken on the FEI Tecnai G^2 F30 transmission electron microscope at an acceleration voltage of 300 kV. AFM (Bruker Dimension® Icon™) was used to characterize the morphology and height of BP-based NSs before and after PEG coating on Si/SiO_2 substrates. UV-vis-NIR absorption spectra were recorded by an Infinite M200 Pro TECAN GENIOS. The optical absorbance per path length (A/L) was determined from the optical absorbance intensity at 808 nm. FTIR were recorded by Thermo Scientific Nicolet iS 50 spectrometer. Raman spectra of PEGylated BP NSs was performed on a high-resolution confocal Raman microscope (HORIBA LabRAM HR800) at room temperature. Size and zeta potential of NSs were performed by Malvern Mastersizer 2000 (Zetasizer Nano ZS90, Malvern Instruments Ltd., UK). The data were gained with the average of three times.

6. Photothermal properties of PEGylated BP NSs. The photothermal heating curves was obtained by monitoring the temperature changes of different solutions under the irradiation of 808 nm NIR laser with power density of 1.0 W/cm^2. The laser was provided by a fiber-coupled continuous semiconductor diode laser (KS-810F-8000, Kai Site Electronic Technology Co., Ltd.) and the temperatures were recorded by an electronic thermometer.

7. Drug loading and *in vitro* release kinetics. Drug loading efficiency was determined by UV-vis-NIR spectra of BP-PEG NSs (50 μg/ml) before and after DOX loading (30, 60, 90, 120, 150, 180 or 210 μg/ml) at different feeding ratios (i.e. DOX/NSs feeding ratio = 0.6, 1.2, 1.8, 2.4, 3, 3.6 or 4.2). Briefly, the absorption peaks at 490 nm was used to determine DOX concentration, after the absorbance contributed from BP-PEG NSs was subtracted from the spectra of BP-PEG/DOX NSs. Similarly, the loading efficiency of Cy7-loaded NSs applied in *in vivo* imaging and biostribution was also determined by UV-vis-NIR spectra of BP-PEG NSs (50 μg/ml) before and after Cy7 (50 μg/ml) loading at the determined Cy7/NSs feeding ratio of

1. The absorption peaks at 750 nm was used to determine Cy7 concentration, after the absorbance contributed from BP-PEG NSs was subtracted from the spectra of BP-PEG/Cy7 NSs. For testing the DOX release kinetics, 1 ml of BP-PEG/DOX NSs (at a DOX/NSs feeding ratio of 3) was packaged in a dialysis bag (MWCO = 14 kDa), then incubated in 19 ml PBS at different pH (pH = 7.4 or 5.0). 1 ml of the outside solution was collected to measure the concentrations of released drugs via absorbance spectrometer, and 1 ml of fresh PBS was added to keep the constant volume. Photothermal-triggered release of DOX studies were performed under the same condition at PH = 5.0, excepet irradiating with an 808 nm NIR laser at a power density of 1 W/cm^2 over a period of 10 min.

8. Cell culture assays. Human cervical cancer cell HeLa, human breast carcinoma cell line MCF-7, human prostate cancer cell line PC3 and human liver cancer cell line HepG2 were from American Type Culture Collection (ATCC, Rockville, MD). HeLa, MCF-7, and HepG2 cells were cultured in normal DMEM medium with 10% FBS and 1% penicillin/streptomycin. PC3 cells were cultured in normal RPMI-1640 medium with 10% FBS and 1% penicillin/streptomycin.

9. *In vitro* toxicity and safety study. HeLa cells were seeded at a density of 5,000 cells/well in 96-well plates and incubated overnight. Afterwards, the cells were incubated with BP NSs, BP-PEG NSs, and BP-PEG-FA NSs at different BP concentration (1, 5, 10, 25, 50, 100 μg/ml) for 24 h, 48 h, and 72 h, respectively (fresh medium with the same BP concentrations were changed every day). Five multiple holes were set for every sample. The formulations were changed with MTT-contained DMEM (5 mg/ml) and an additional 4 h-incubation was conducted for the cells at a determined time. Then MTT was removed and DMSO was dropped in to dissolve the formazan crystals at 37 °C (dark, 2 h). A microplate reader (Bio-Rad Model 680, UK) was used to measure the absorbance at 570 nm. Untreated cells represented for 100%

viability and cells incubated with MTT-free medium were taken as blank to calibrate the spectrophotometer to zero absorbance. Similar experiments were carried out on MCF-7, HepG2, and PC3 cells to further evaluate the safety of PEGylated BP NSs. These cells were incubated with BP-PEG NSs at different BP concentrations (5, 10, 25, 50, 100 μg/ml) for 48 h. then MTT assay performed.

10. *In vitro* cellular targeting assays. The *in vitro* cellular targeting effect of BP-PEG-FA NSs was investigated by a FCM study. Briefly, HeLa cells were incubated with BP-PEG/DOX NSs or BP-PEG-FA/DOX NSs (60 μg/ml BP-PEG or BP-PEG-FA, 50 μg/ml DOX) at 37 °C for 1 h, respectively. The cells were collected and washed with PBS, and the intracellular fluorescence of DOX was detected by FCM after excitation at 488 nm.

11. *In vitro* photothermal therapy study. HeLa cells were incubated with BP NSs, BP-PEG NSs, and BP-PEG-FA NSs (10, 25, and 50 μg/ml) for 4 h at 37 ºC under the same conditions and then irradiated by an 808 nm laser (1.0 W/cm^2) for 10 min. The area of each well was fully covered by the laser spot. After additional incubation for 12 h, the relative cell viabilities were then measured by the MTT assay. The cell viability was normalized by control group without any treatment.

12. *In vitro* chemotherapy study. HeLa cells were incubated with free DOX, BP-PEG/DOX NSs and BP-PEG-FA/DOX in 96-well plates for 24 h at different DOX concentrations (0, 2.5, 5, 12.5, 25, 50, and 100 μg/ml). Afterwards, the cells were washed with PBS, the standard cell viability MTT assay was carried out to determine the cell viabilities relative to the control cells incubated with the same volume of PBS.

13. Plasmid and transfection. The Rab genes in T Vector were kindly provided by Prof. Jiahuai Han and subsequently sub-cloned into DsRed-C1 and EGFP-C1 vectors. The DsRed-LC3 and EGFP-LC3 plasmids were cloned in our laboratory. The plasmids were transiently transfected into HeLa cells with the participation of Lipofectamine 2000 (Invitrogen) according to the manufacturer's instructions.

14. Cellular uptake of PEGylated BP NSs: Non-transfected or DsRed-Rabs transfected HeLa cells were incubated with BP-PEG-FITC NSs (60 μg/ml) at 37 °C for 4 h. Then the cells were washed with PBS, fixed by 4% paraformaldehyde for 15min and stained with DAPI for 10 min. Finally, the cellular uptake of NSs was examined by confocal laser scanning microscopy (Olympus FV1000-81, Tokyo, Japan).

15. Immunoblotting. Briefly, cell lysates were resolved on 12% SDS-PAGE and analyzed by immunoblotting using LC3 and P62 primary antibodies, followed by enhanced chemiluminescence detection.

16. Immunofluorescence. For abbreviation, the HeLa cells were washed with PBS, fixed by 4% paraformaldehyde for 15 min, permeabilized by 0.01% Triton-100 for 2 min. Then, the cells were incubated with the promary antibodies: Clathrin, Flotillin, Cdc42, RhoA, Caveolin, Arf6, EEA1, LC3 and P62. Finally, the FITC and Alexa Fluor 647 labbeled secondary antibodies were used to detect the primary antibodies.

17. *In vitro* combined antitumor therapy. To study the *in vitro* combined therapy of PEGylated BP NSs, the viability of HeLa cells were tested by MTT assays via different types of treatment as follow. i) PTT groups: 4 h-incubation with BP-PEG NSs (or BP-PEG-FA NSs) then irradiated with an 808 nm NIR laser at 1.0 W/cm^2 for 10 min; ii) PTT-Biological response

combined therapy groups: 30 μM free CQ pretreated HeLa cells for 24 h, then irradiated with an 808-nm NIR laser at 1.0 W/cm^2 for 10 min after 4 h-incubation with BP-PEG NSs (or BP-PEG-FA NSs); iii) Triple response combined therapy: 30 μM free CQ-pretreated HeLa cells for 24 h, then irradiated with an 808 nm NIR laser at 1.0 W/cm^2 for 10 min after 4 h-incubation with BP-PEG/DOX NSs (or BP-PEG-FA/DOX NSs). HeLa cells treated with only BP-PEG NSs or free CQ (30 μM) was used as control. A series of BP-PEG or BP-PEG-FA NSs concentrations (5, 10, and 25 μg/ml) was used in this study, DOX concentration was 5 μg/ml.

18. Xenograft tumor model. The female severe combined immunodeficient (SCID) nude mice were provided by the Institute of Laboratory Animal Sciences, Chinese Academy of Medical Science. The Administrative Committee on Animal Research in Tsinghua University approved the protocols for all animal assays in this paper. About 100 μl of HeLa cells in DMEM medium were implanted subcutaneously into the backs of mice (~20 g) at a dosage of 2×10^6 cells per mouse. After that, we observed the tumor growth in each mouse at frequent intervals. The tumor size and tumor volume (V) was calculated as $4\pi/3 \times (\text{length}/2) \times (\text{width}/2)^2$ by a vernier caliper. 95% of the mice injected developed a tumor with an average volume of about 100 mm^3 after two weeks.

19. Pharmacokinetic studies. For *in vivo* pharmacokinetic study, normal BALB/c mice (n = 5 per group) were *i.v.* injected with 200 μl free 6 mg/kg DOX or BP-PEG/DOX NSs (7.1 mg/kg BP-PEG, 6 mg/kg DOX) through the tail vein. At each time point (0.5, 1, 2, 4, 8, 12, and 24 h), 20 μl of blood was collected from the mouse and then dissolved in 300 μl of lysis buffer (1% SDS, 1% Triton-100, 40 mM Tris acetate, 10 mM EDTA and 10 mM DTT). 300 μl of HCl/isopropanol was added to extract DOX from blood. The mixture was then incubated in dark overnight. After centrifuged to obtain the DOX in supernatant, the amount of DOX remaining in blood was determined by absorbance. Similarly, The absorption peaks at 490 nm

was used to determine DOX concentration, after the absorbance contributed from background and BP-PEG NSs were subtracted from the spectra.

20. *In vivo* imaging and biodistribution analysis. Tumor bearing mice were randomly divided into two groups (n = 3 mouse per group), i.e. BP-PEG/Cy7 NSs group and BP-PEG-FA/Cy7 NSs group (1 mg/kg equivalent Cy7 for NSs) and *i.v.* injected with 200 μl dye-loaded NSs via tails. A Maestro™ Automated In-Vivo Imaging system (CRi Maestro™, USA) was used to take the in vivo images of mice at 1, 12, and 24 h post-injection respectively. NIR light with a central wavelength at 704 nm was used as the excitation source. Furthermore, mice were humanely killed at 24 h post-injection, and then the heart, liver, spleen, lung, kidney and tumor were collected from each mouse without delay. The fluorescence intensity in all organs was further analyzed by the Maestro™ Automated In-Vivo Imaging system. The fluorescence intensity (a.u.) was quantified by Image-J.

21. *In vivo* test for biological response-induced therapy. Tumor bearing nude mice were *i.v.* injected with 200 μl of Saline (Group 1), 7.1 mg/kg BP-PEG NSs (Group 2), and 7.1 mg/kg BP-PEG NSs together with intratumoral (i.t.) injection of CQ (50 mg/kg) in PBS (Group 3). After 24 h injection, the nude mice were irradiated with 808 nm laser at 1 W/cm^2 for 10 min. During the course of irradiation, we utilized an IR thermal camera to monitor the temperature changes of the tumor sites. Group 1 was taken as control.

22. *In vivo* combined antitumor effects. When the tumor size reached approximately 150 mm^3 (designed as Day 0), treatment was performed. Two experienced researchers randomly divided the mice into seven groups (n = 5 per group), which were *i.v.* injected 50 mg/kg CQ (as biological response-induced therapy control, Group 2), 6 mg/kg DOX (as chemotherapy control, Group 3), BP-PEG-FA/DOX NSs (as chemotherapy with delivery platform group; 7.1 mg/kg

for NSs and 6 mg/kg for DOX, Group 4), 7.1 mg/kg BP-PEG-FA NSs (as PTT group, Group 5), BP-PEG-FA NSs (7.1 mg/kg) together with *i.t.*-injected 50 mg/kg CQ (as PTT + biological response induced therapy group, Group 6), and BP-PEG-FA/DOX (7.1 mg/kg for NSs and 6 mg/kg for DOX) together with *i.t.*-injected 50 mg/kg CQ (as combined triple-response therapy group: chemotherapy + PTT + biological response induced therapy, Group 7) in 200 μl PBS on Day 0, 4, 8, 12. Saline was used as control. Group 5, 6 and 7 were treated with 808 nm laser at 1 W/cm^2 for 10 min at tumor sites after 24 h injection. The body weight and tumor size of each mouse were recorded every other day. The mice were humanely killed after two weeks of treatment and all the tumors were collected from each group.

23. Hematocylin and eosin (H&E) stained histology. For the H&E stained histology, healthy Balb/c mice were administered daily *i.v.* injection of (i) Saline, (ii) BP-PEG-FA NSs (7.1 mg/kg), (iii) BP-PEG-FA NSs (7.1 mg/kg) + CQ (50 mg/kg), or (iv) BP-PEG-FA/DOX NSs (7.1 mg/kg for NSs, 6 mg/kg for DOX) + CQ (50 mg/kg). After two weeks of treatment, all mice were humanely killed and the organs were harvested, fixed in a 10% formalin solution, and embedded in paraffin for H&E staining.

24. Blood routine test. The *in vivo* toxicity PEGylated BP NSs was preliminarily evaluated by a blood routine test (BRT). In brief, BP-PEG NSs (10 mg/kg) was *i.v.* injected into fifteen healthy Balb/c mice in three groups. After 1, 7, and 14 days injection, all five mice in a group were sacrificed to collect blood (0.8 ml) for BRT, respectively. Five other healthy Balb/c mice without any treat were used as the controls.

25. Statistical analysis. All results are reported as the mean ± S.E.M. and comparisons were performed using a two tailed Student's t test. All experiments, unless otherwise stated, were

performed in triplicate. Statistical values are indicated in figures according to the following scale: * P<0.05, ** P<0.01 and *** P<0.001.

Results and discussions

1. Photothermal properties of PEGylated BP NSs

Considering the attractive photothermal properties of BP-based QDs and BP-based NPs reported very recently,[2, 3] we have good reasons to believe the BP-based NSs could be promisingly applied in PTT of cancer, although there have no report on the PTT of BP-based NSs up to now. The extinction and photothermal properties of BP-PEG NSs were further confirmed in our study. The surface PEG coating had little influence on the UV-vis-NIR absorbance of BP NSs (Figure S9a). As shown in Figure S9b, a broad absorption band from the ultraviolet (UV) to the NIR regions could be observed in the UV–vis–NIR absorbance spectra of BP-PEG NSs at different BP concentrations (300, 200, 100 and 50 μg/ml), which were quite similar to those of other 2D nanomaterials such as graphene oxide (GO) and WS_2.[4, 5] According to the Lambert-Beer law (A/L = αC, where A, L, and C are Absorbance value, the path length and the BP concentration respectively), the extinction coefficient α was calculated to be 15.9 $L \cdot g^{-1} \cdot cm^{-1}$ at λ= 808 nm. The extinction coefficient of BP-PEG NSs is about 4.4 times larger than that of GO NSs (3.6 $L \cdot g^{-1} \cdot cm^{-1}$),[4] and 4.1 times larger than that of Au nanorods (3.9 $L \cdot g^{-1} \cdot cm^{-1}$) [2] previously reported, which are both common photothermal agents widely used in recent studies. Although the extinction coefficient of BP-PEG NSs is lower than that of WS_2 NSs,[5] the application of ultrathin BP-PEG NSs as phototeramal agents is very tempting. In order to evaluate the photothermal properties of these BP-based NSs, the aqueous BP-PEG NSs solutions with low concentrations (5, 50, 100 μg/ml) were exposed to an 808 nm NIR laser at power density of 1.0 W/cm^2. The temperatures of different BP-PEG NSs solutions were then measured as a function of time (Figure S10). At a relatively low BP concentration of 100 μg/ml, the BP-PEG NSs solutions showed a good photothermal effect with the temperature

increment of 24.6 °C after irradiation for 10 min. With a strong contrast, the temperature change of water had only a rise of 3.3 °C, demonstrating the BP-PEG NSs had a rapid and effective ability converting the NIR light into thermal energy. Notably, compared with the reported BP-PEG NPs (~10-20 nm in hydrodynamic size),[3] the NS structure of BP in our study showed a much lower concentration to reach the similar temperature increment (100 μg/ml v.s. 700 μg/ml), which may be attributed to the ultrathin 2D structure and high surface area of BP-PEG NSs. Moreover, the photothermal conversion efficiency of BP-PEG NSs was calculated to be approximately 29.8% according a reported method.[3, 6] As presented in our study, this conversion efficiency was higher than that of Au-based nanomaterials (13% for nanoshells and 21% for nanorods),[7] that of Cu_3BiS_3 (27.4%),[8] and that of $Cu_{2-x}Se$ (22%).[9] A high photothermal stability of BP-PEG NSs was further confirmed by a heating-cooling cycle assay and a time-variable experiment using the same BP-PEG NSs solution via recording the change of temperatures under irradiation with an 808 nm NIR laser at power density of 1.0 W/cm^2 (Figure S11). To this end, the excellent photothermal properties of BP-PEG NSs have been well-verified.

2. *In vitro* toxicity study of PEGylated BP NSs

Due to the biocompatibility and the toxicity of the nanomaterials are the major concern for their bio-applications, we investigated the intrinsic toxicity of BP-based NSs via standard methyl thiazolyl tetrazolium (MTT) assays before further moving on to in vitro cellular studies. As presented in our results, there was no obvious cytotoxicity observed in HeLa cells for all BP-based NSs (e.g. BP NSs, BP-PEG NSs and BP-PEG-FA NSs) at different concentrations (1, 5, 10, 25, 50, 100 μg/ml) from 24 h to 72 h (Figure S16). We further checked the toxicity of BP-PEG NSs on some major types of cancer cells (i.e. cervical cancer HeLa cells, breast cancer MCF-7 cells, liver cancer HepG2 cells, prostate cancer PC3 cells), similar low toxicity of BP-PEG NSs could be confirmed in all types of cancer cells at different concentrations (5, 10, 25,

50, 100 μg/ml) for 48 h (Figure S17). Our results suggested the excellent suitability of BP-based NSs for their biomedical applications.

3. In vivo biological response assays

After confirmation that the PEGylated BP NSs could be systemic administration, we continued to design a preliminary experiment to test the *in vivo* effect of this biological response-induced therapy, since the *in vitro* effect for CQ-mediated inhibition of lysosomes and autophagy (i.e. biological response-induced therapy) was well-demonstrated and we need to check this before final *in vivo* combined therapy. Tumor bearing nude mice were *i.v.* injected with 200 μl of Saline (as control), 200 μl of BP-PEG NSs (7.1 mg/kg), and 200 μl of BP-PEG NSs (7.1 mg/kg) together with intratumoral (*i.t.*) injection of 50 mg/kg CQ. After 24 h injection, the nude mice were irradiated with the 808 nm laser at 1 W/cm^2 for 10 min. During the course of irradiation, we utilized an IR thermal camera to monitor the temperature changes of the tumor sites (Figure S31a). As presented in our studies, the temperature change of the tumor sites for Saline group was only increased by 5-6 °C after 10 min of irradiation (Figure S31b). However, more significant temperature increase could be noticed for BP-PEG NSs group (~ 12 °C) and BP-PEG NSs together with *i.t.* injected CQ (~ 16 °C). These results indicated that PEGylated BP NSs could induce a good *in vivo* photothermal effect and the CQ-mediated response may inhibit the degradation of PEGylated BP NSs *in vivo*, which would contribute to the relatively higher temperature BP-PEG NSs together with *i.t.* injected CQ.

4. In vivo toxicity evaluation

Finally, we carried out a BRT study to verify the potential *in vivo* safety of our PEGylated BP NSs. Clinical BRT is the most common used medical technology to monitor the health condition and disease detection of human beings worldwide, which would have guiding significance for further biomedical application of the PEGylated BP theranostic delivery

platform. Female and healthy Balb/c mice were *i.v.* injected with BP-PEG NSs and euthanized for blood collection after 1, 7, and 14 days. The blood of untreated healthy Balb/c mice were used as control. BRT were then carried out at Peking University Shenzhen Hospital. Encouragingly, almost all BRT parameters of the BP-PEG NSs treated mice were very close to those of healthy mice in control group (Figure S33), demonstrating the PEGylated BP NSs may not be toxic at the tested dose during the treatment period in our preliminary *in vivo* toxicity studies.

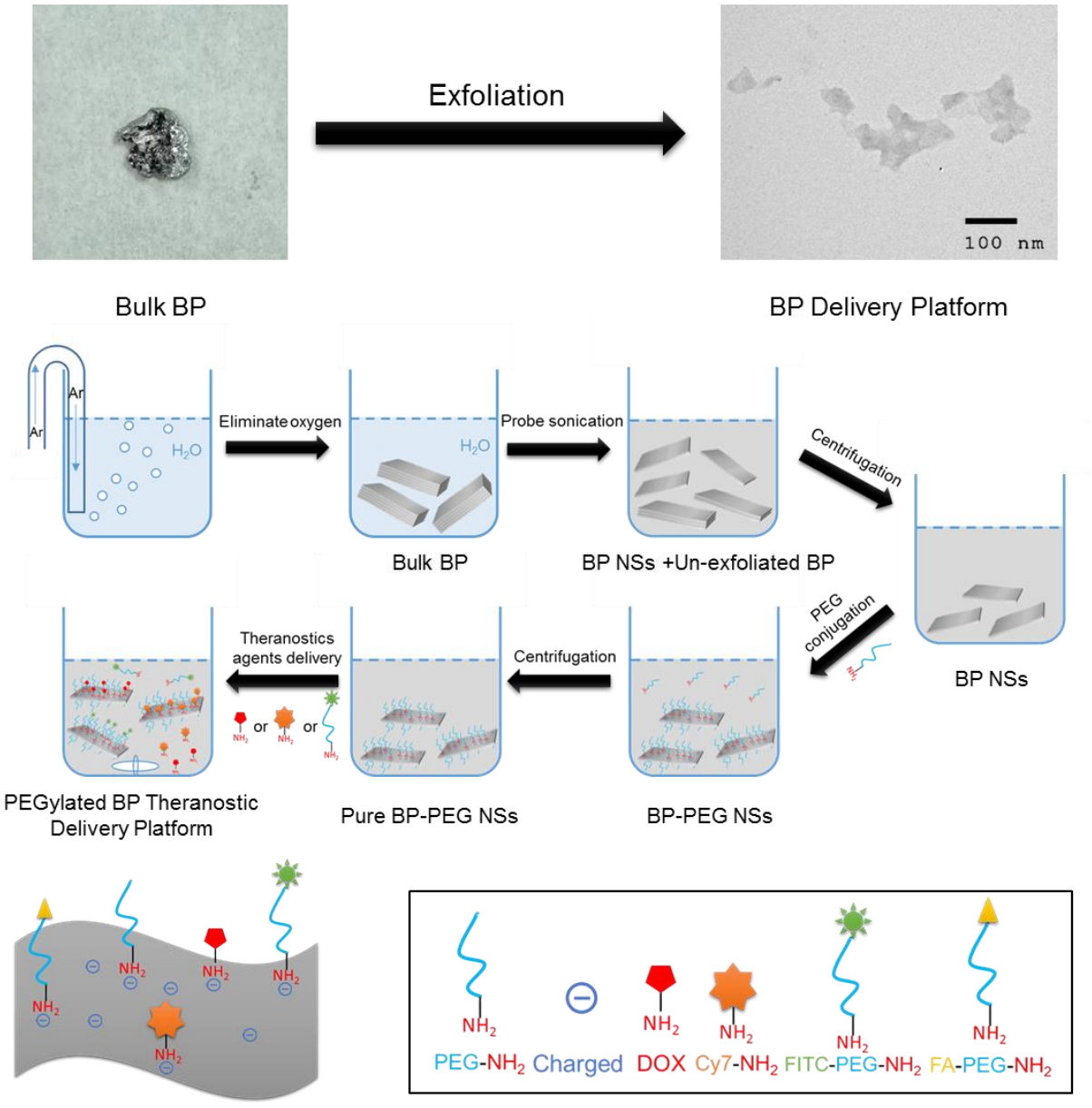

Supporting Figure S1. Schematic illustration for the mechanical exfoliation of bulk BP into ultrathin BP NSs in water and preparation of PEGylated BP theranostic delivery platform. The theranostic agents were loaded on the surface of BP-PEG NSs via strong electrostatic adsorption.

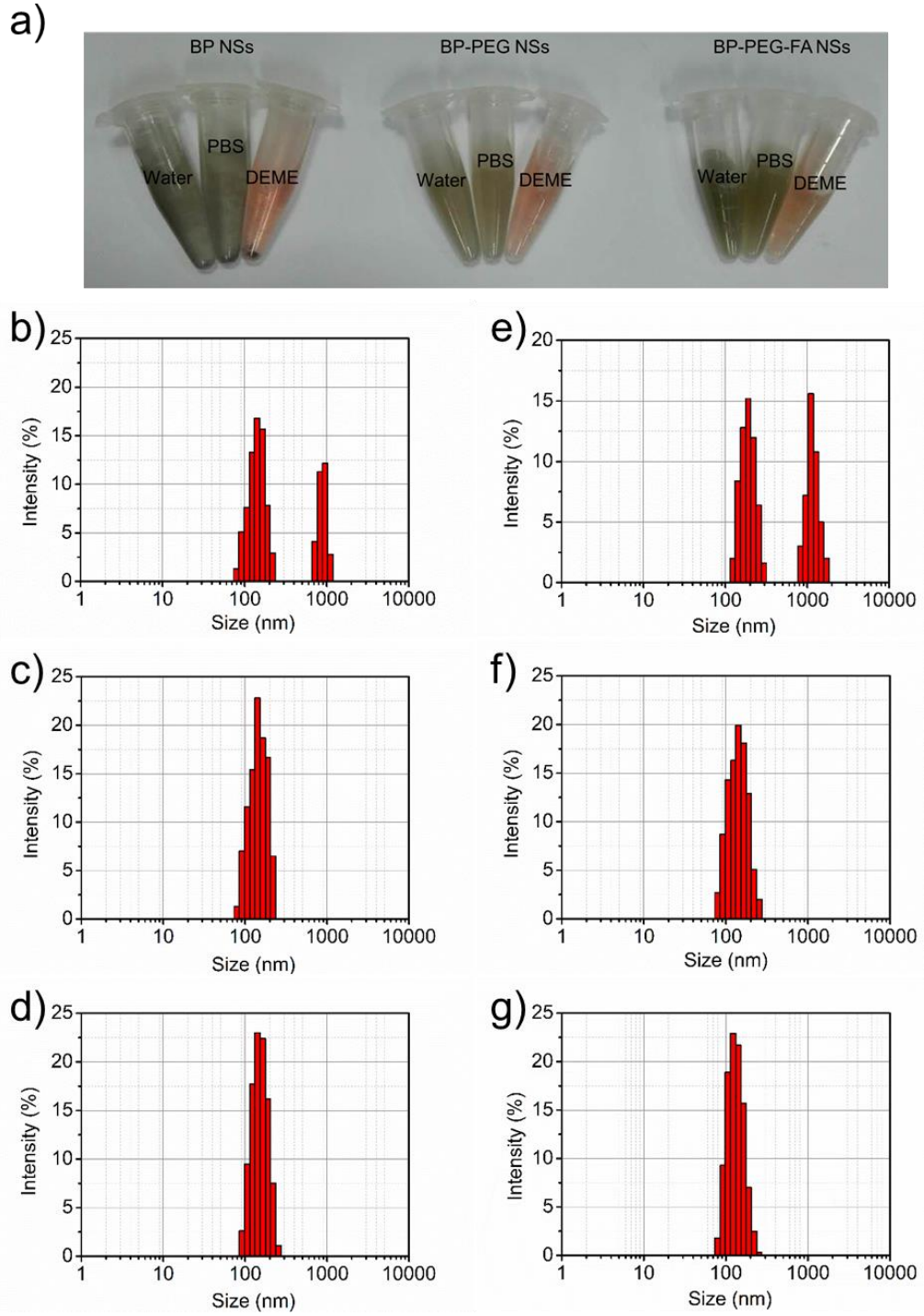

Supporting Figure S2. (a) Photos of BP NSs, BP-PEGNSs, and BP-PEG-FA NSs in H_2O, PBS and cell culture medium after 1 week-standing. (b) DLS size distribution of as-made BP NSs, BP-PEG NSs and BP-PEG-FA NSs in (b-d) PBS and (e-g) DMEM with 10% serum.

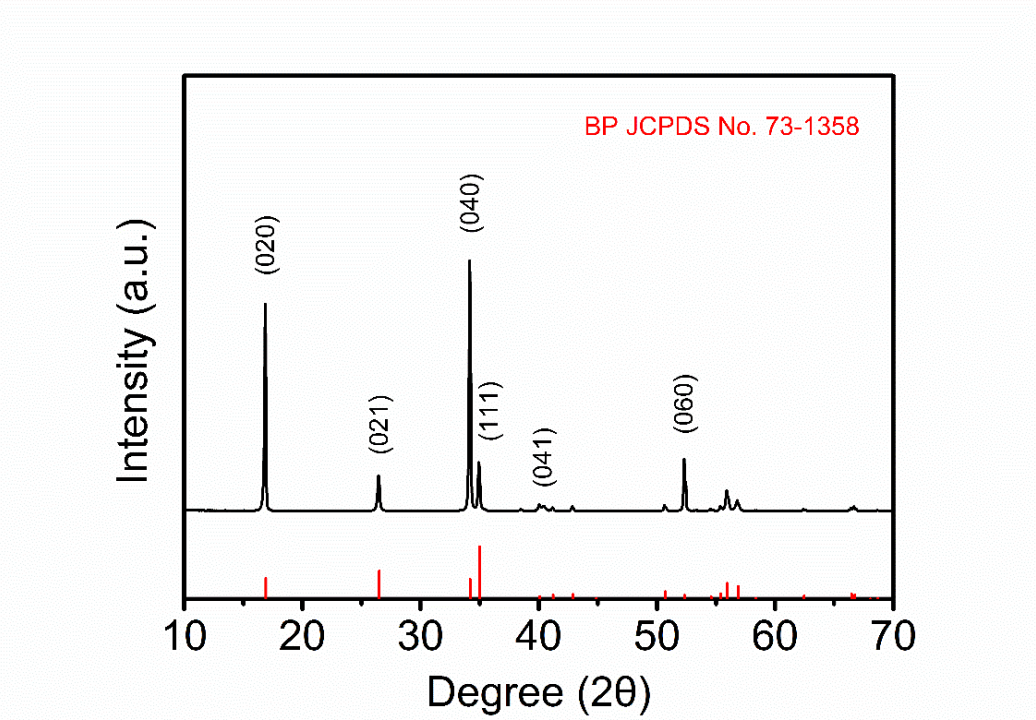

Supporting Figure S3. XRD pattern of BP-PEG NSs.

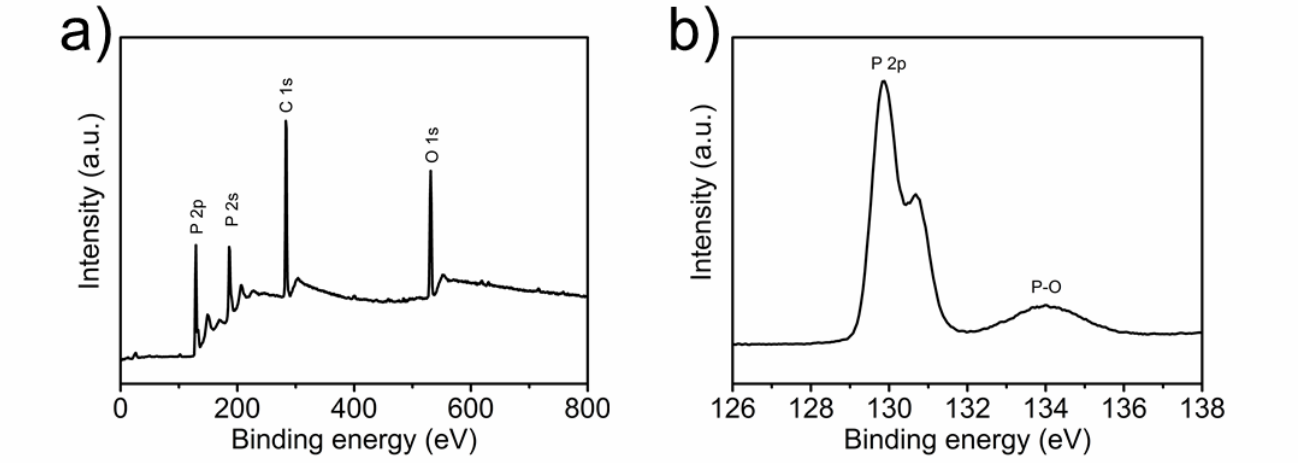

Supporting Figure S4. XPS spectra of BP-PEG NSs: (a) Survey spectrum. (b) P2p spectrum.

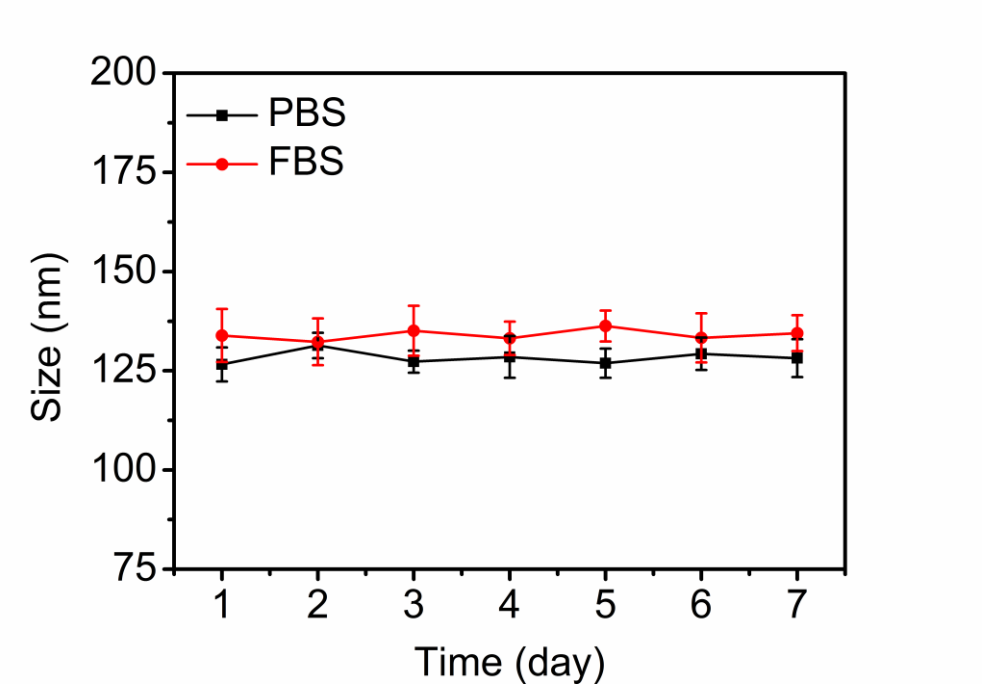

Supporting Figure S5. Stability of BP-PEG NSs in PBS and FBS, respectively, by monitoring particle size over a span of 7 days.

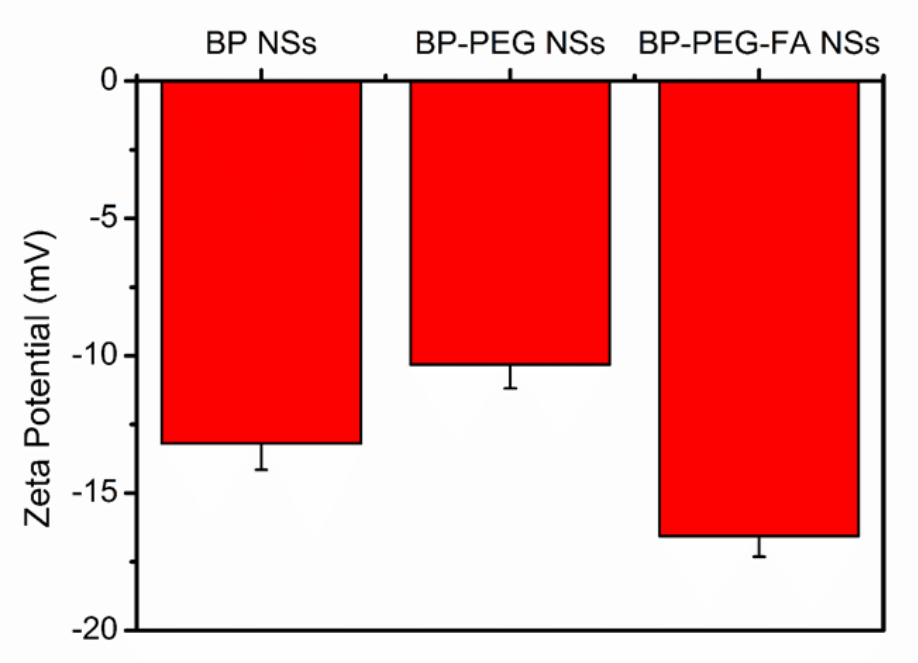

Supporting Figure S6. Zeta potentials of BP NSs before and after PEGylation in PBS (pH = 7.4).

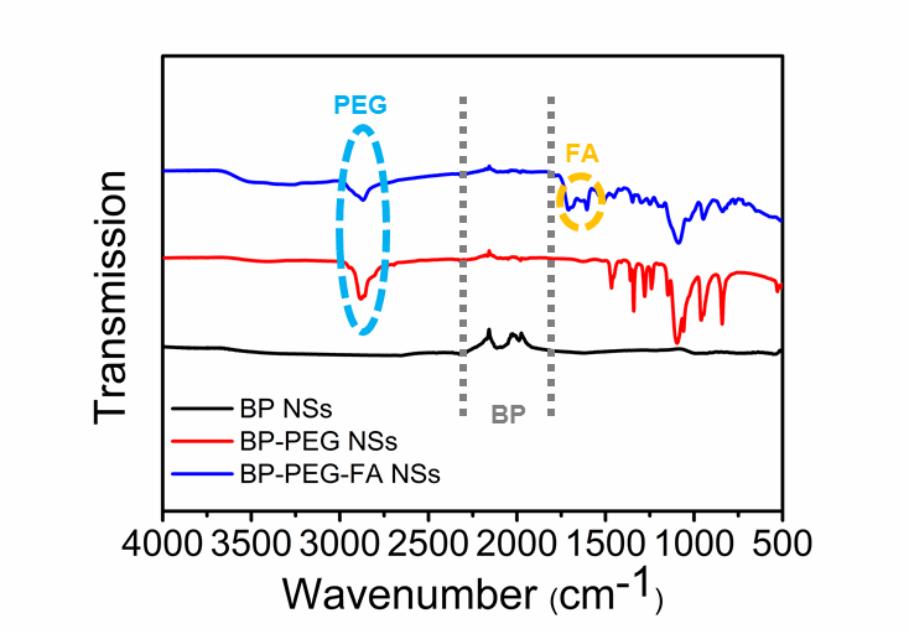

Supporting Figure S7. FT-IR spectra of BP NSs, BP-PEG NSs, and BP-PEG-FA NSs. The IR absorption band at ~2900 cm^{-1} in the BP-PEG sample was attributed to the CH vibration in PEG. Characteristic stretching vibration at ~1637-1653 cm^{-1} was attributed to the amide bonding within FA structure. The converse peaks between ~1800 cm^{-1} and ~2300 cm^{-1} could be contributed to the unique structure of multilayer BP.

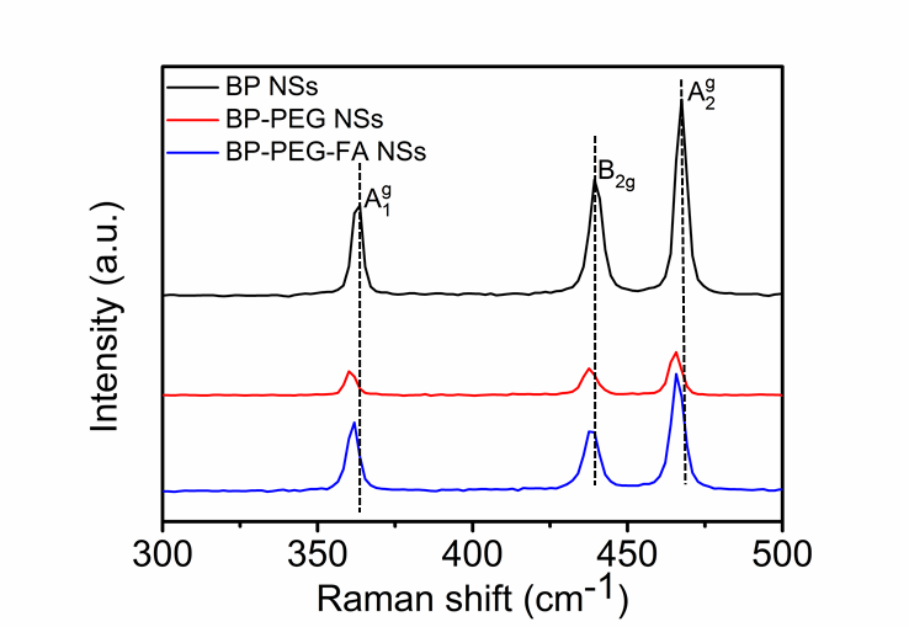

Supporting Figure S8. Raman spectr a of exfoliated BP NSs, BP-PEG NSs, and BP-PEG-FA NSs. A slightly shift toward low wavenumber could be found in PEGylated BP NSs.

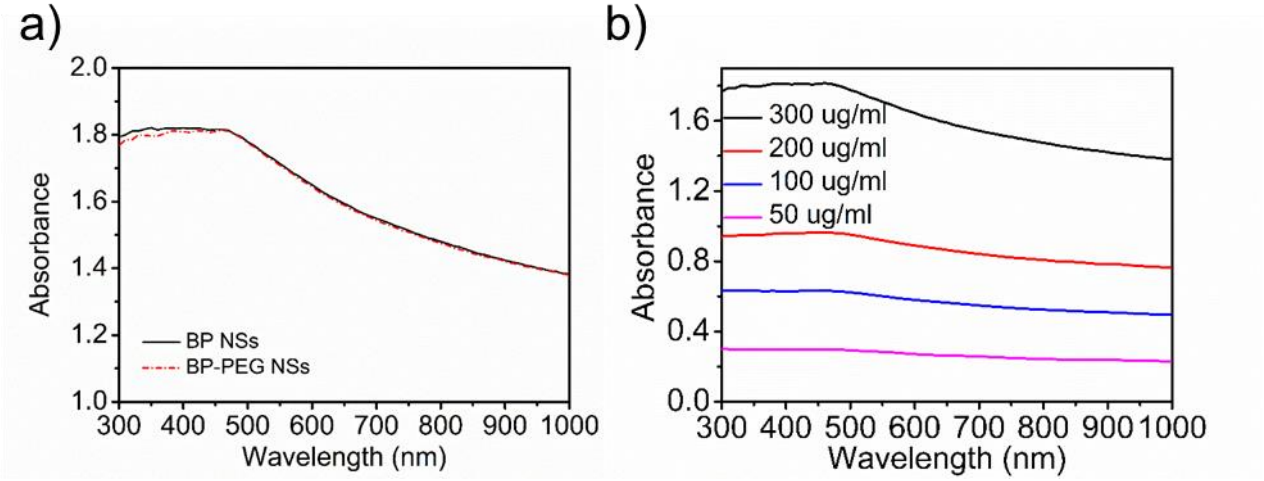

Supporting Figure S9. UV–vis–NIR absorbance spectra of (a) BP NSs and BP-PEG NSs. (b) BP-PEG NSs at different BP concentrations.

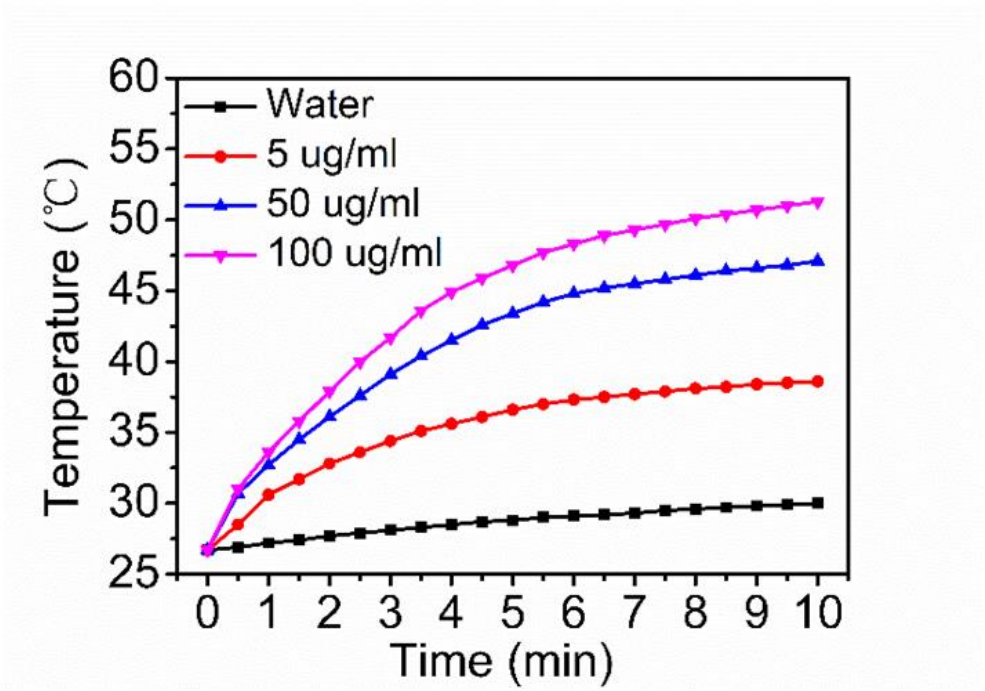

Supporting Figure S10. Photothermal heating curves of pure water and a BP-PEG NSs solution under 808 nm laser irradiation (1.0 W/cm^2) at different BP concentration for 10 min.

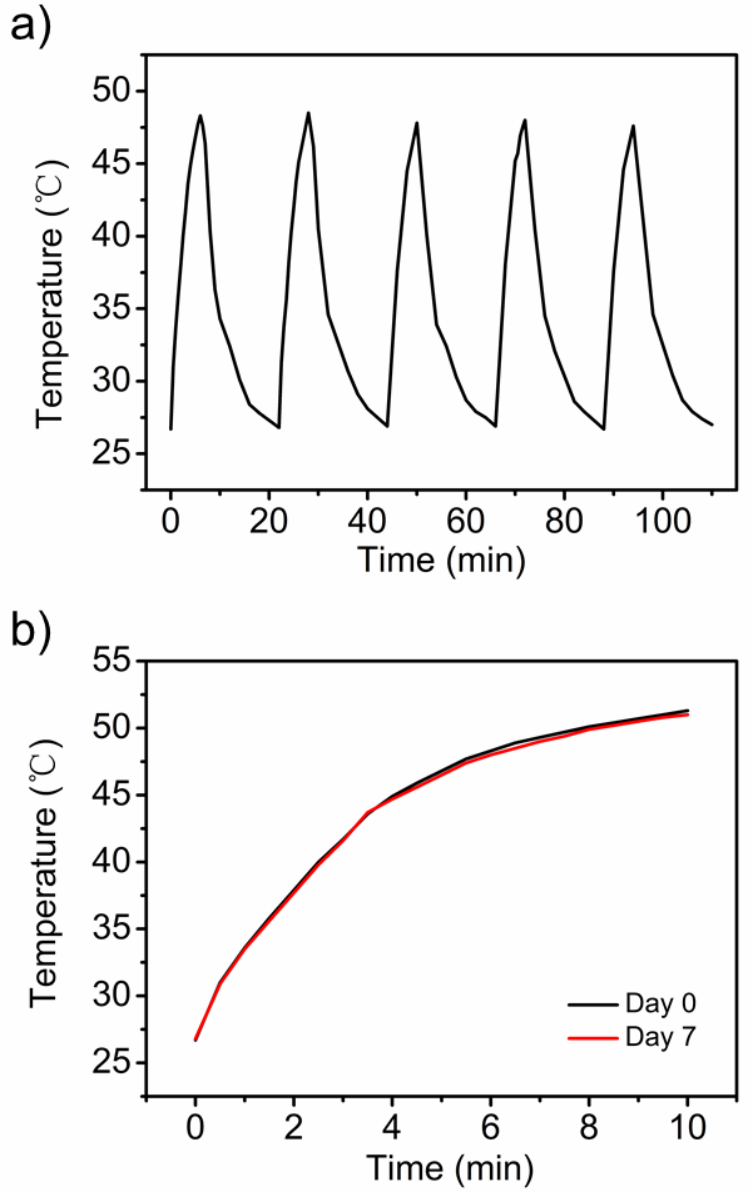

Supporting Figure S11. Photothermal stability of BP-PEG NSs (BP concentration at 100 μg/ml). (a) Heating of a suspension of the BP-PEG NSs in water for five laser on/off cycles with an 808 nm NIR laser at power density of 1.0 W/cm^2. (b) The change of temperature of BP-PEG NSs in water before and after one week standing (stored at 4 °C) irradiated under an 808 nm NIR laser at power density of 1.0 W/cm^2.

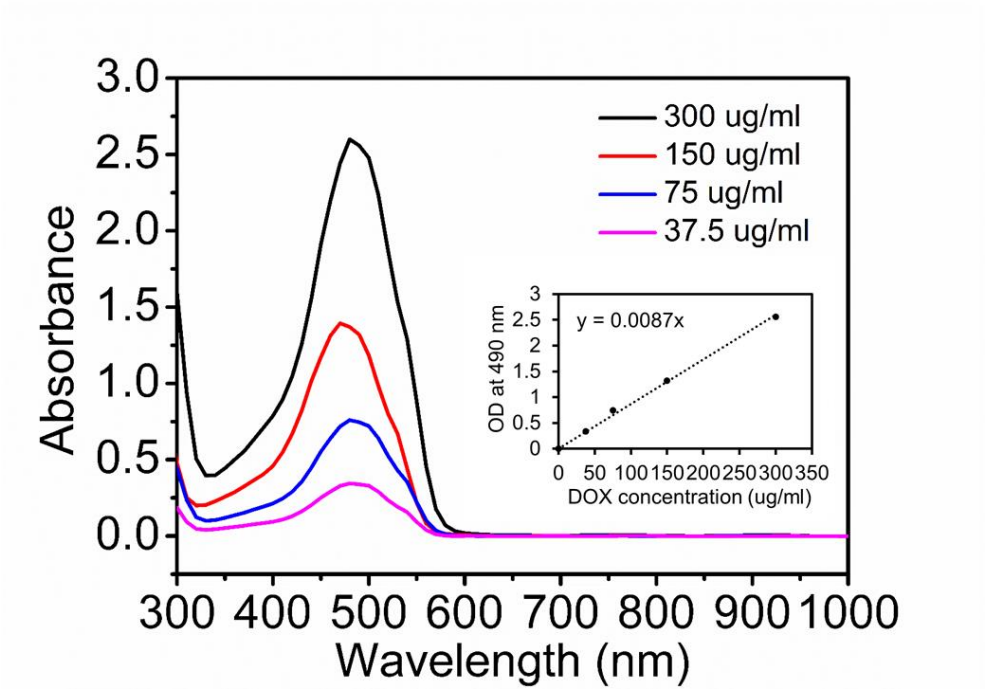

Supporting Figure S12. Absorbance spectra of DOX in water at different concentrations (300, 150, 75 and 37.5 μg/ml). Inset: Normalized absorbance at different DOX concentration for λ = 490 nm.

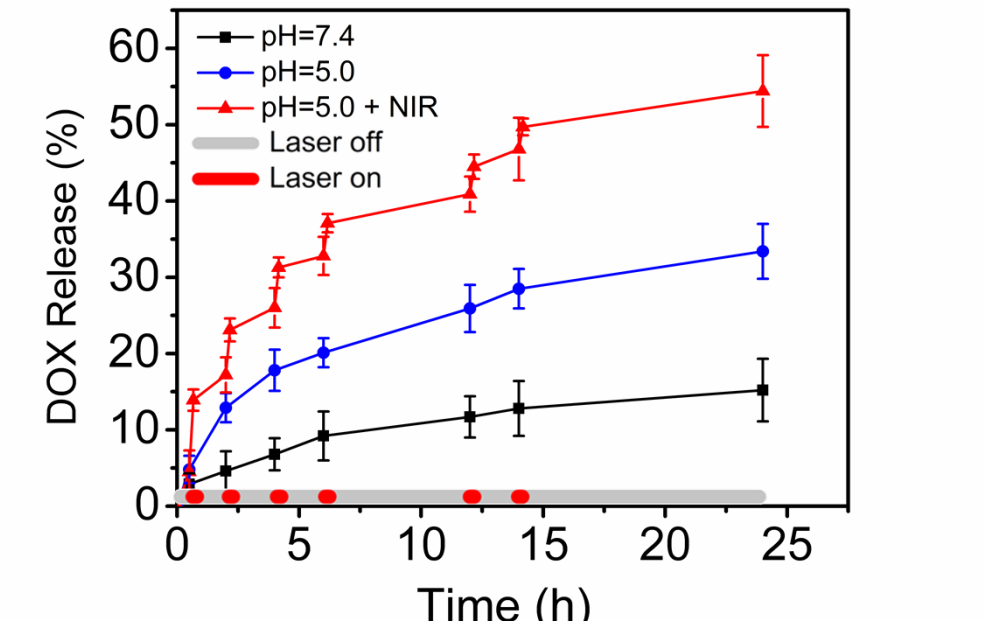

Supporting Figure S13. Drug release kinetics of BP-PEG/DOX NSs at pH = 7.4 and pH = 5.0 (in the absence or presence of 1.0 W/cm^2 NIR laser).

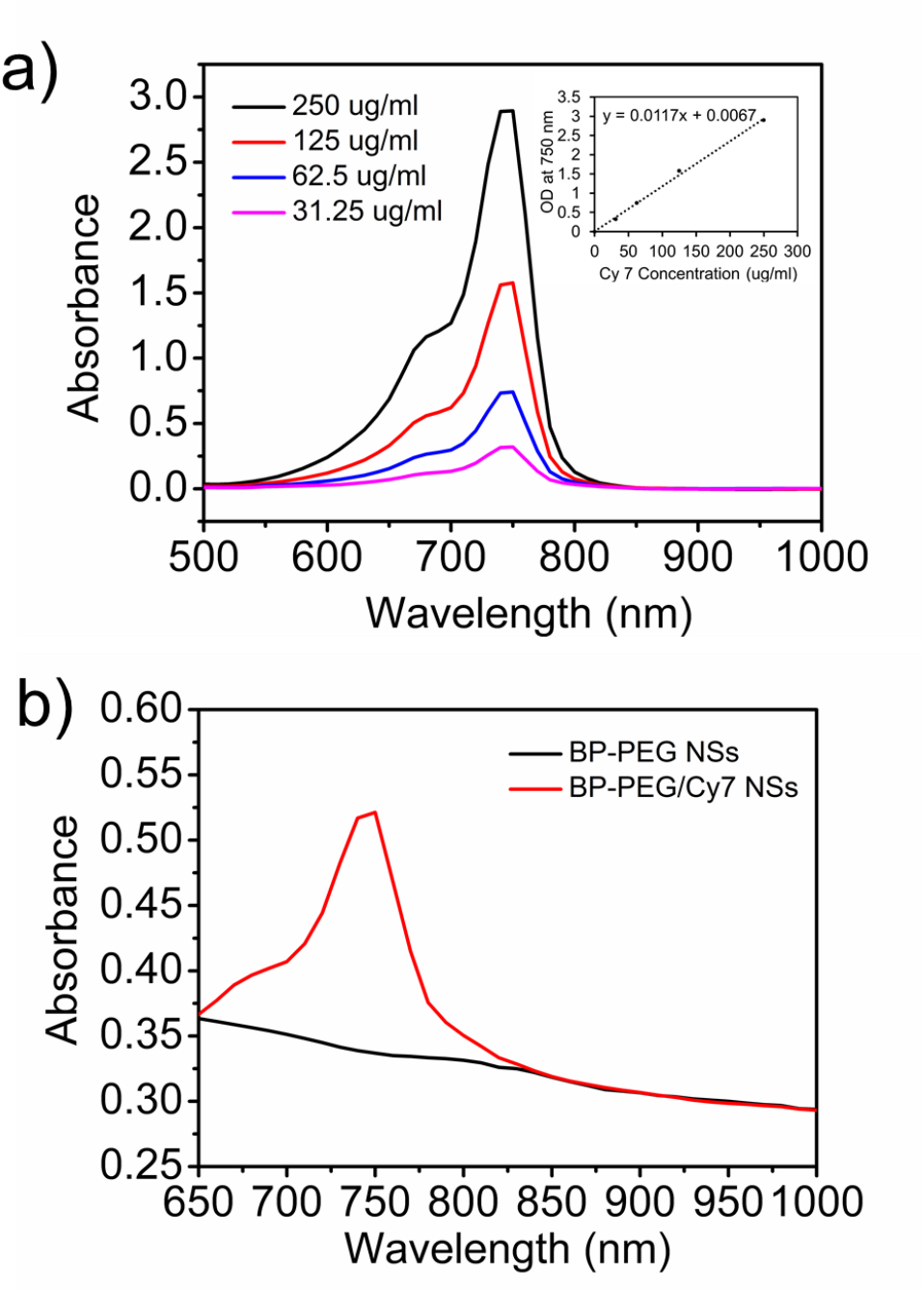

Supporting Figure S14. Absorbance spectra of (a) Cy7 in water at different concentrations (250, 125, 62.5 and 31.25 μg/ml) and (b) purified BP-PEG/Cy7 after Cy7 (50 μg/ml) interacted with BP-PEG NSs (50 μg/ml) in water. The Cy7 loading efficiency was calculated to be 30.38% (w/w%) at the Cy7/NSs feeding ratio of 1. Inset: Normalized absorbance at different Cy7 concentration for λ = 750 nm.

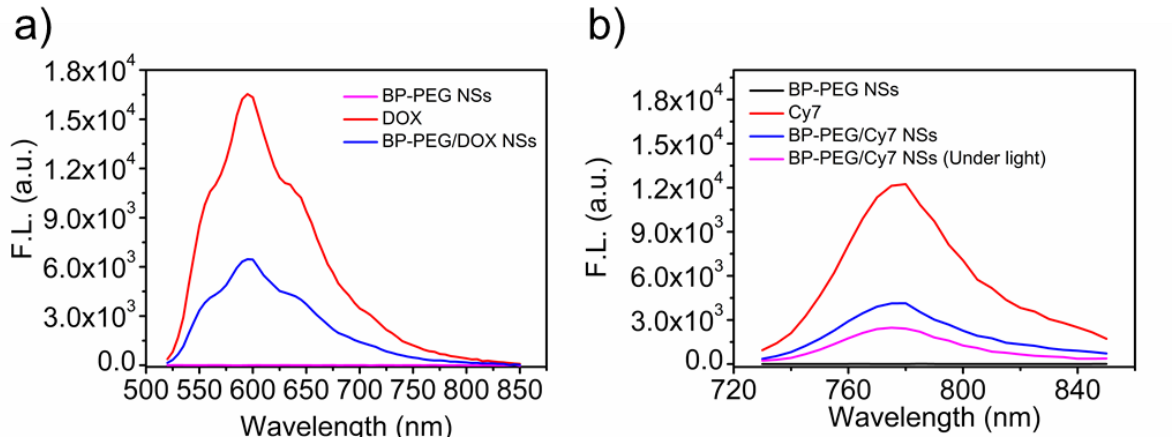

Supporting Figure S15. Fluorescence quenching of molecules after loading onto BP-PEG NSs. (a) Fluorescent spectra of DOX (54 μg/ml), BP-PEG NSs (50 μg/ml), and BP-PEG/DOX NSs (54 μg/ml DOX, 50 μg/ml BP-PEG NSs) aqueous solutions (λex = 490 nm). (b) Fluorescent spectra of Cy7 (15.2 μg/ml), BP-PEG NSs (50 μg/ml), and BP-PEG/Cy7 NSs (15.2 μg/ml Cy7, 50 μg/ml BP-PEG NSs; avoiding light *v.s.* under light) aqueous solutions (λex = 704 nm).

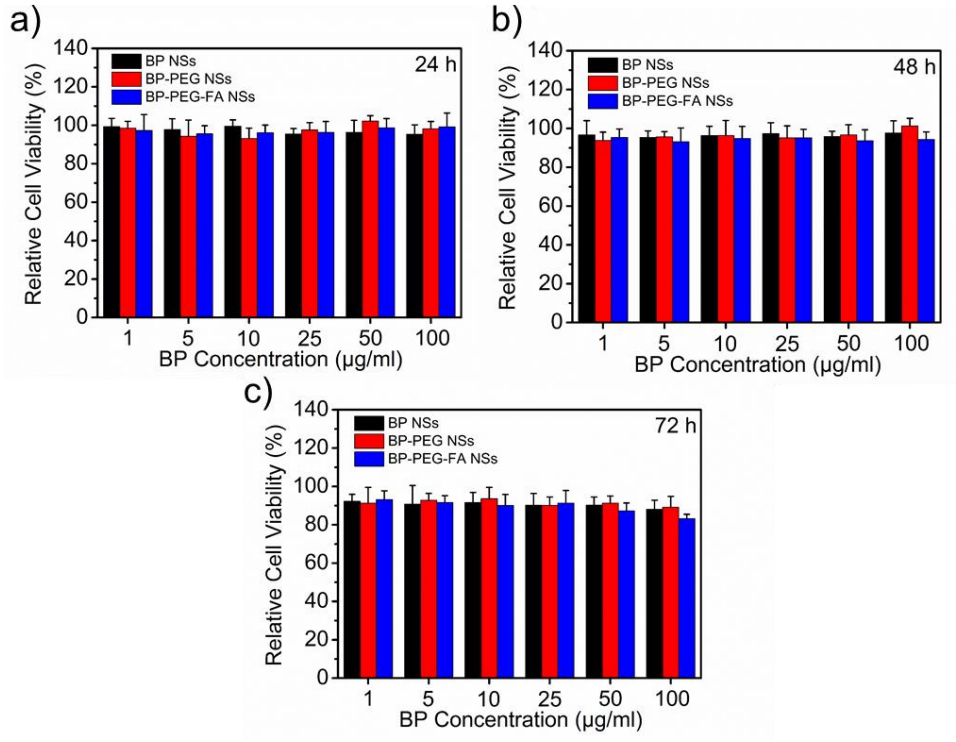

Supporting Figure S16. Relative viabilities of HeLa cells after incubation with various concentrations (1, 5, 10, 25, 50, and 100 μg/ml) of BP NSs, BP-PEG NSs and BP-PEG-FA NSs for (a) 24 h, (b) 48 h, and (c) 72 h.

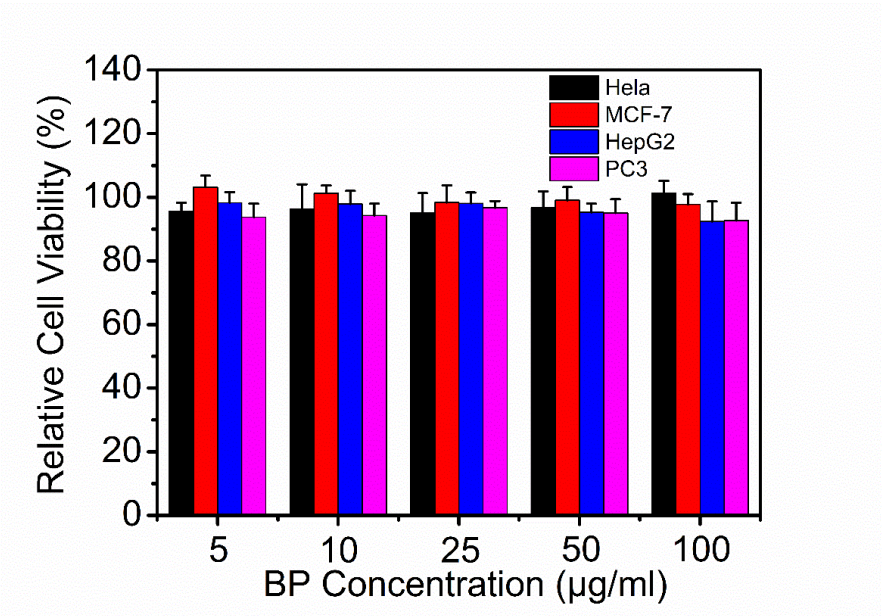

Supporting Figure S17. Relative viabilities of different cancer cells (HeLa, MCF-7, HepG2 and PC3 cells) after incubation with various concentrations (5, 10, 25, 50, and 100 μg/ml) of BP-PEG NSs for 48 h.

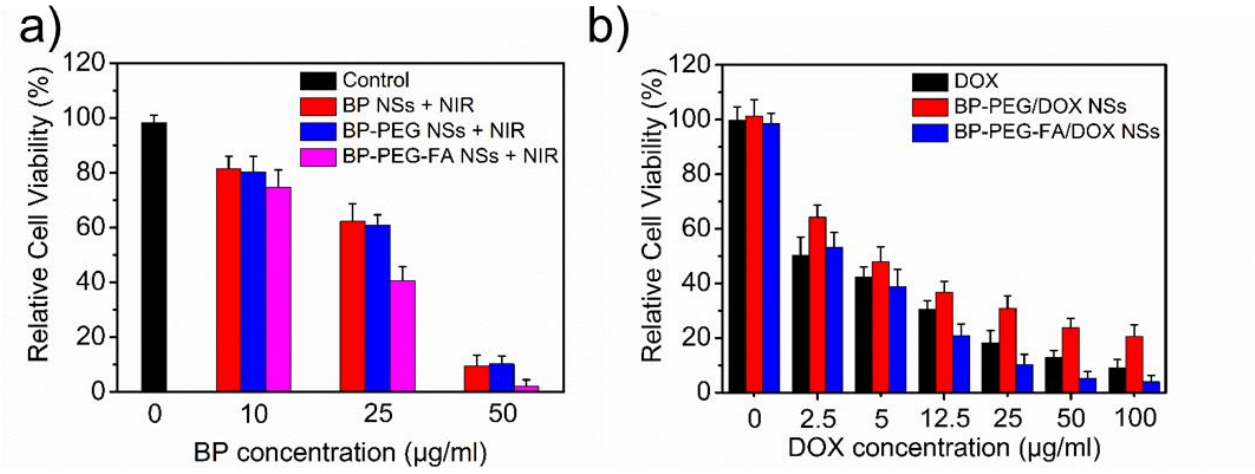

Supporting Figure S18. *In vitro* PTT and chemotherapy of PEGylated BP NSs. (a) Relative viabilities of HeLa cells after 4 h-incubation with BP-based NSs (10, 25, and 50 μg/ml) and irradiation with an 808 nm laser at 1.0 W/cm^2 for 10 min. The cell viability was normalized by control group without any treatment. (b) Relative viabilities of HeLa cells after 24 incubation with free DOX, BP-PEG/DOX NSs, or BP-PEG-FA/DOX NSs at various concentrations (0, 2.5, 5, 12.5, 25, 50, and 100 μg/ml).

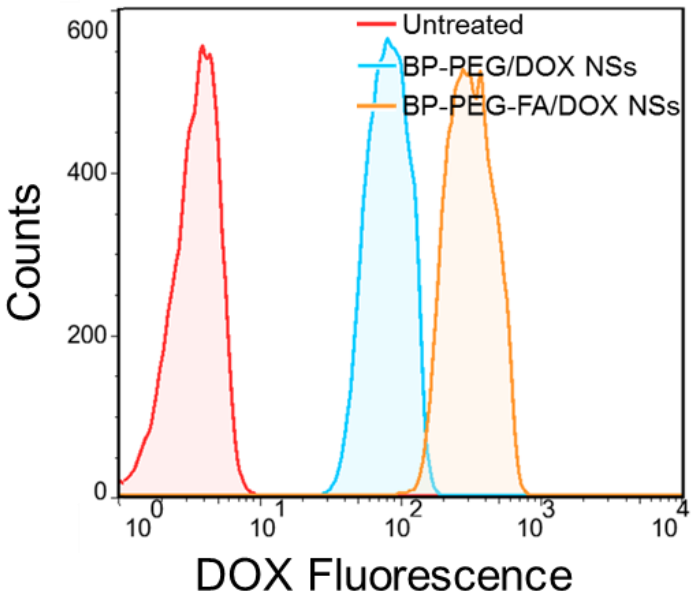

Supporting Figure S19. Flow cytometry (FCM) histogram profiles of cellular DOX fluorescence intensities in HeLa cells after 1 h-incubation with BP-PEG/DOX NSs and BP-PEG-FA/DOX NSs.

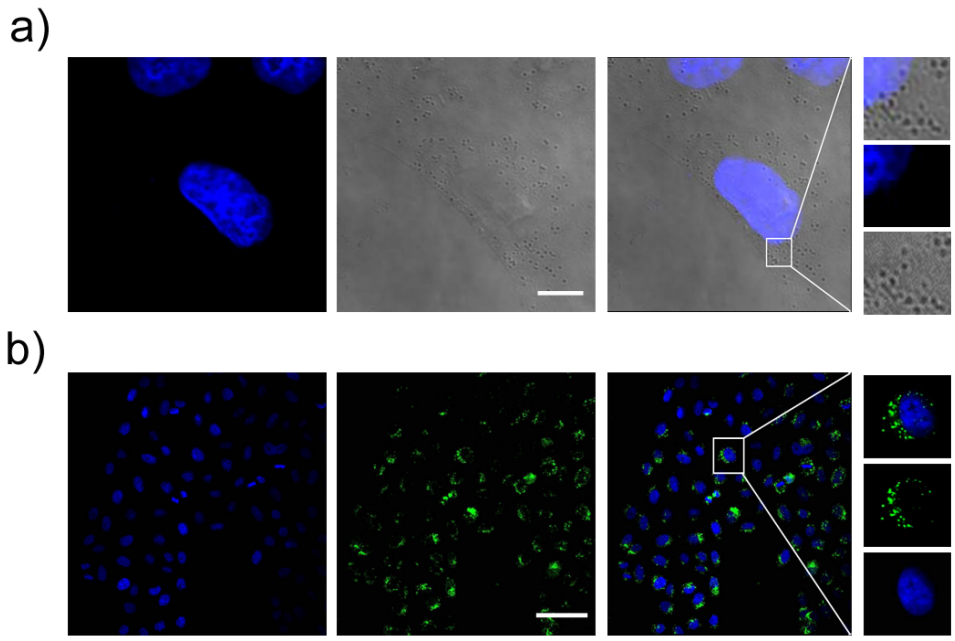

Supporting Figure S20. Cellular uptake of BP-PEG-FITC NSs after 4 h-incubation with HeLa cells. (a) Bright-field images (scale bar, 5 μm) and (b) Fluorescent images were performed (scale bar, 50 μm).

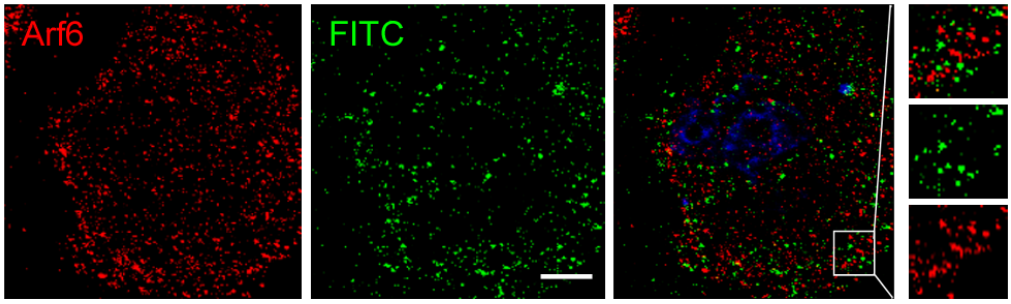

Supporting Figure S21. Confocal images of HeLa cells for Arf6-independent pathway test of BP-PEG-FITC NSs (Scale bar, 5 μm). HeLa cells were treated with BP-PEG-FITC NSs for 4 h and then Arf6 was detected with primary antibodies against Arf6.

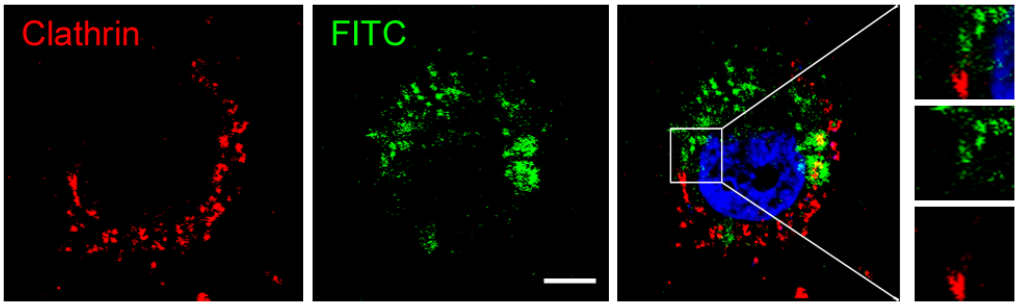

Supporting Figure S22. Confocal images of HeLa cells for clathrin-independent pathway test of BP-PEG-FITC NSs (Scale bar, 5 μm). HeLa cells were treated with BP-PEG-FITC NSs for 4 h and then clathrin was detected with primary antibodies against clathrin.

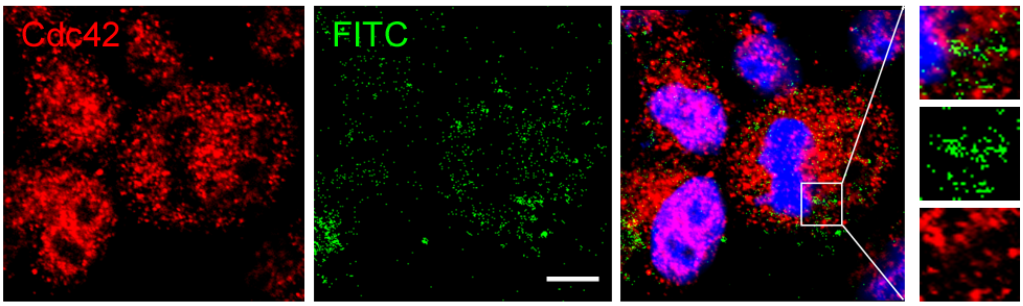

Supporting Figure S23. Confocal images of HeLa cells for Cdc42-independent pathway test of BP-PEG-FITC NSs (Scale bar, 5 μm). HeLa cells were treated with BP-PEG-FITC NSs for 4 h and then Cdc42 was detected with primary antibodies against Cdc42.

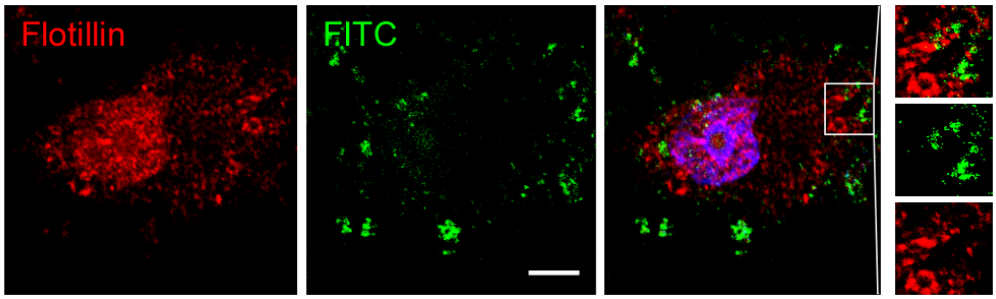

Supporting Figure S24. Confocal images of HeLa cells for flotillin-independent pathway test of BP-PEG-FITC NSs (Scale bar, 5 μm). HeLa cells were treated with BP-PEG-FITC NSs for 4 h and then flotillin was detected with primary antibodies against flotillin.

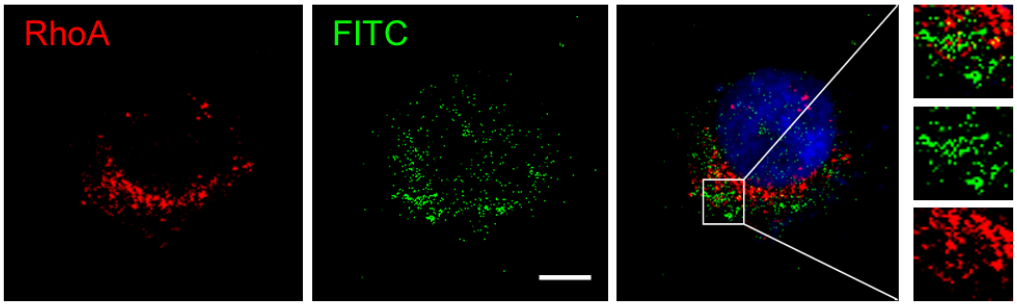

Supporting Figure S25. Confocal images of HeLa cells for RhoA-independent pathway test of BP-PEG-FITC NSs (Scale bar, 5 μm). HeLa cells were treated with BP-PEG-FITC NSs for 4 h and then RhoA was detected with primary antibodies against RhoA.

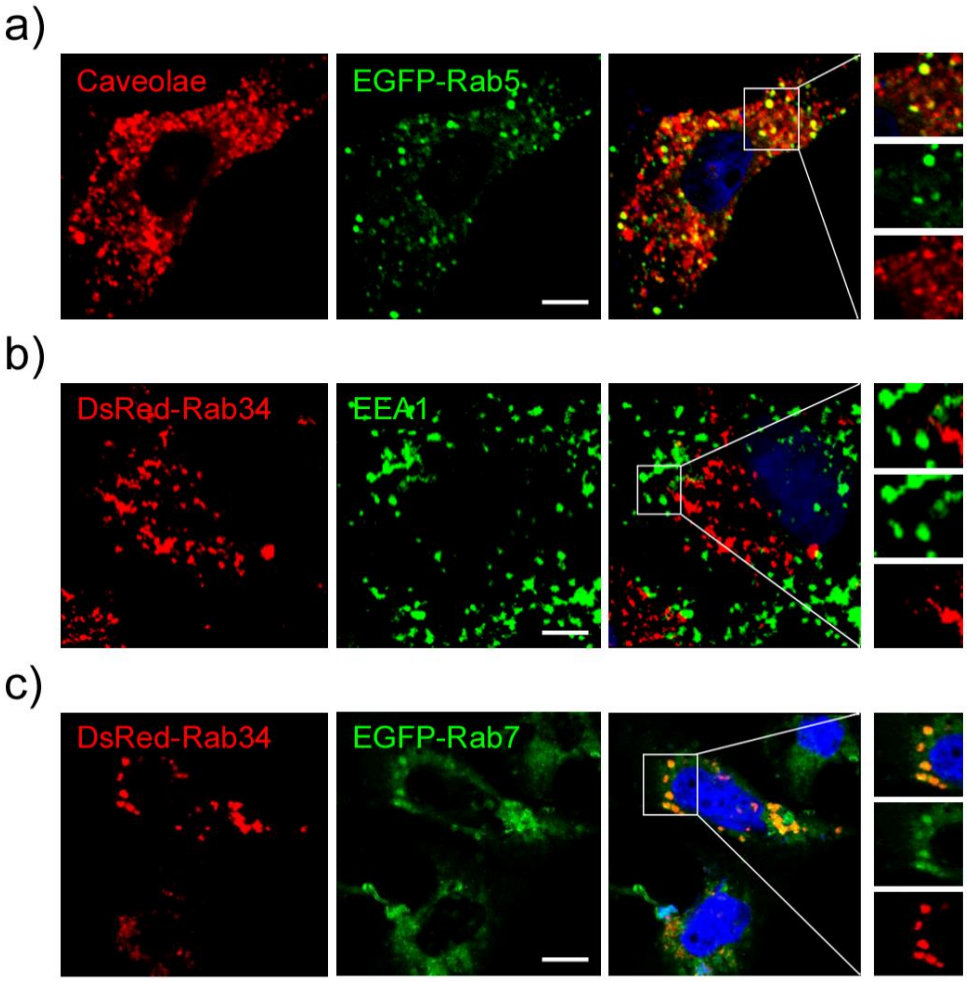

Supporting Figure S26. The co-localization between caveolae & early-endodome, and co-localization between DsRed-Rab34 & late-endosome (Scale bar, 5 μm). (a) Caveolae was detected in EGFP-Rab5 transfected HeLa cells with primary antibodies against caveolae. (b) EEA1 was detected in DsRed-Rab34 transfected HeLa cells with primary antibodies against EEA1. (c) DsRed-Rab34 and EGFP-Rab7 were co-transfected in HeLa cells and then the confocal image was performed.

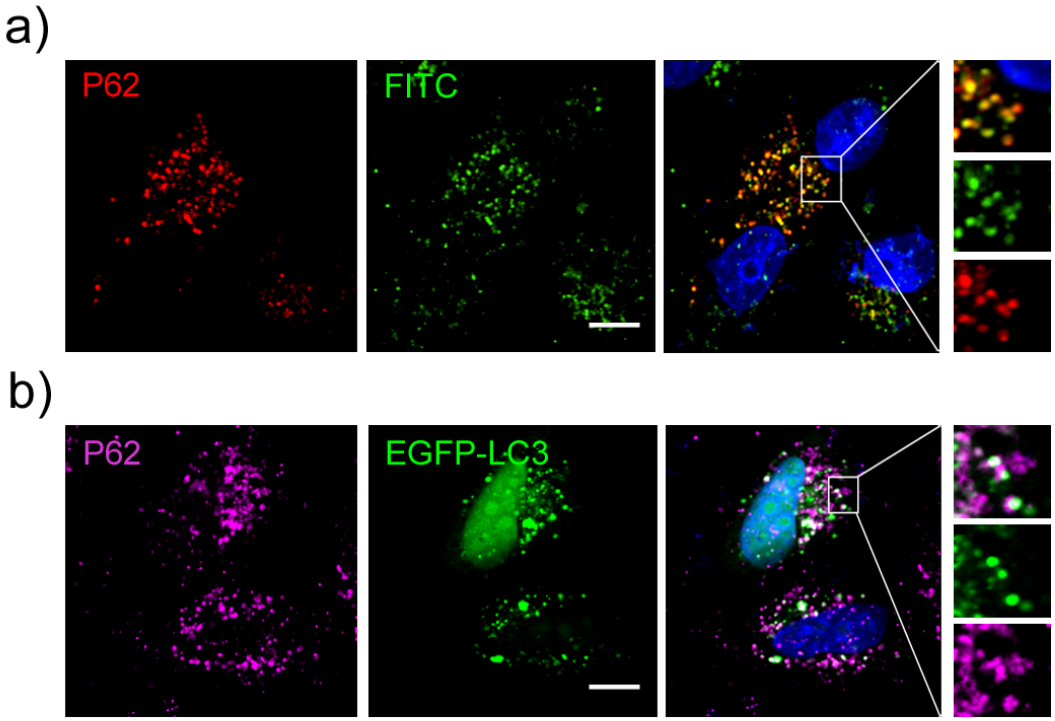

Supporting Figure S27. Sequestosome1 selects PEGylated BP NSs (Scale bar, 5 μm). (a) HeLa cells were treated with BP-PEG-FITC NSs for 4 h and then P62 was detected with primary antibodies against P62. (b) P62 was detected in the EGFP-LC3 transfected HeLa cells with primary antibodies against P62.

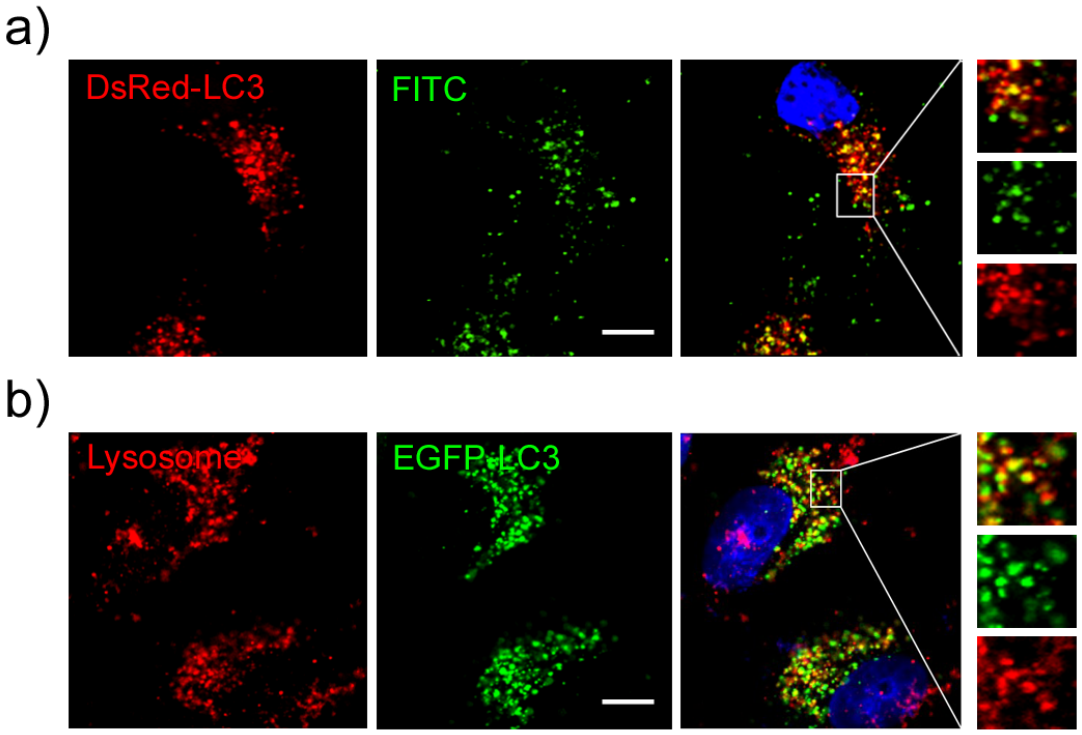

Supporting Figure S28. Autophagysome targets PEGylated BP NSs (Scale bar, 5 μm). (a) DsRed-LC3 transfected HeLa cells were treated with BP-PEG-FITC NSs for 4 h and then confocal imaging was performed. (b) EGFP-LC3 transfected HeLa cells were treated with Lyso-Tracker probes for 30 min and then confocal image was performed.

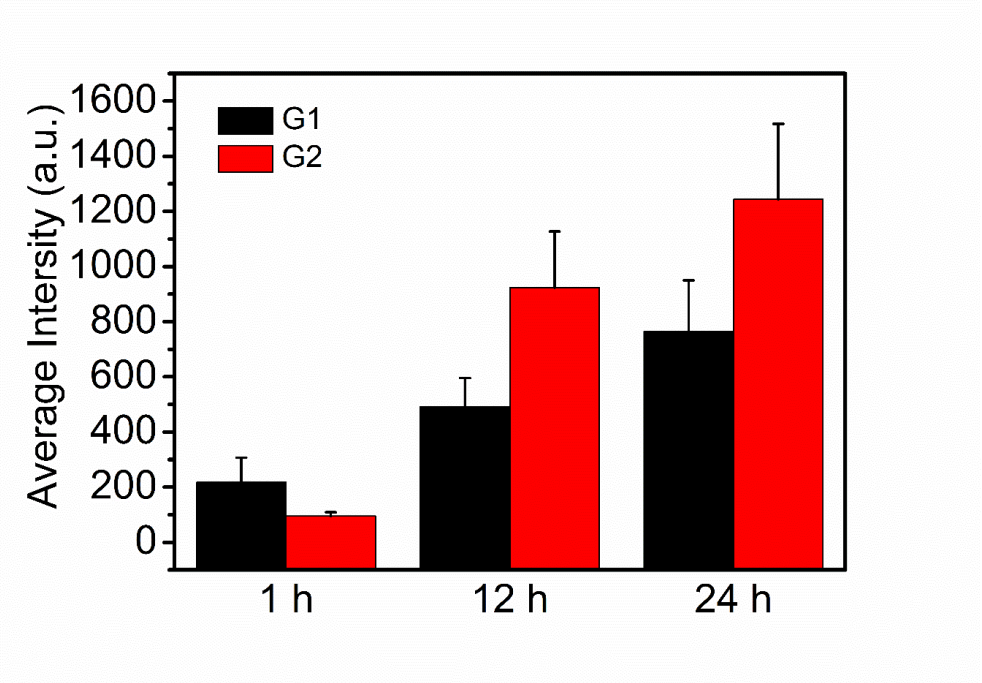

Supporting Figure S29. NIR fluorescence intensity of tumors was quantified at indicated time points (1 h, 12 h, and 24 h). G1: BP-PEG/Cy7 NSs Group; G2: BP-PEG-FA/Cy7 NSs Group.

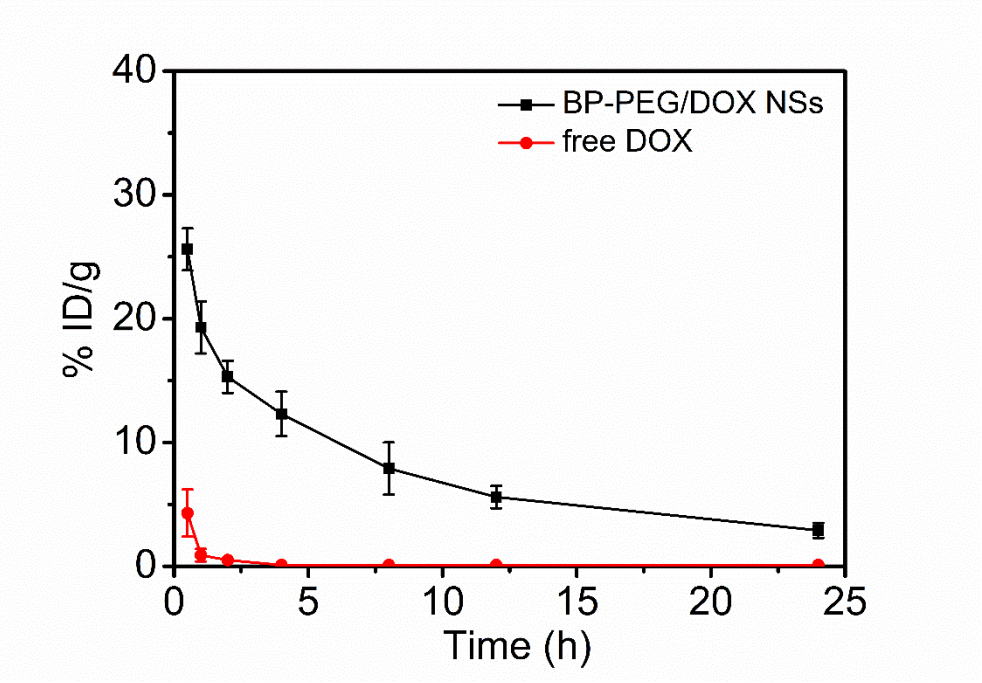

Supporting Figure S30. Blood circulation of free DOX and BP-PEG/DOX NSs after *i.v.* injection. The absorption peaks at 490 nm was used to determine DOX concentration, after the absorbance contributed from background and BP-PEG NSs were subtracted from the spectra.

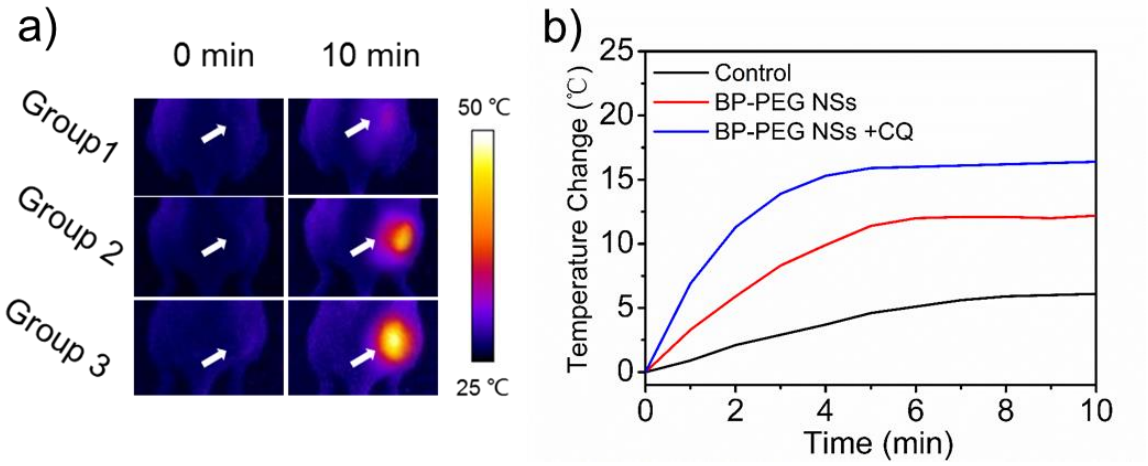

Supporting Figure S31. (a) Thermal images of nude mice bearing HeLa xenograft tumor model after injection of Saline (Group 1), BP-PEG NSs (Group 2), and BP-PEG NSs together with i.t. injected CQ (Group 3), followed by exposure to 808 nm laser irradiation (1.0 W/cm^2, 10 min) after 24 h injection. (b) Tumor temperature changes of nude mice bearing HeLa xenograft tumor models during laser irradiation as indicated in (a).

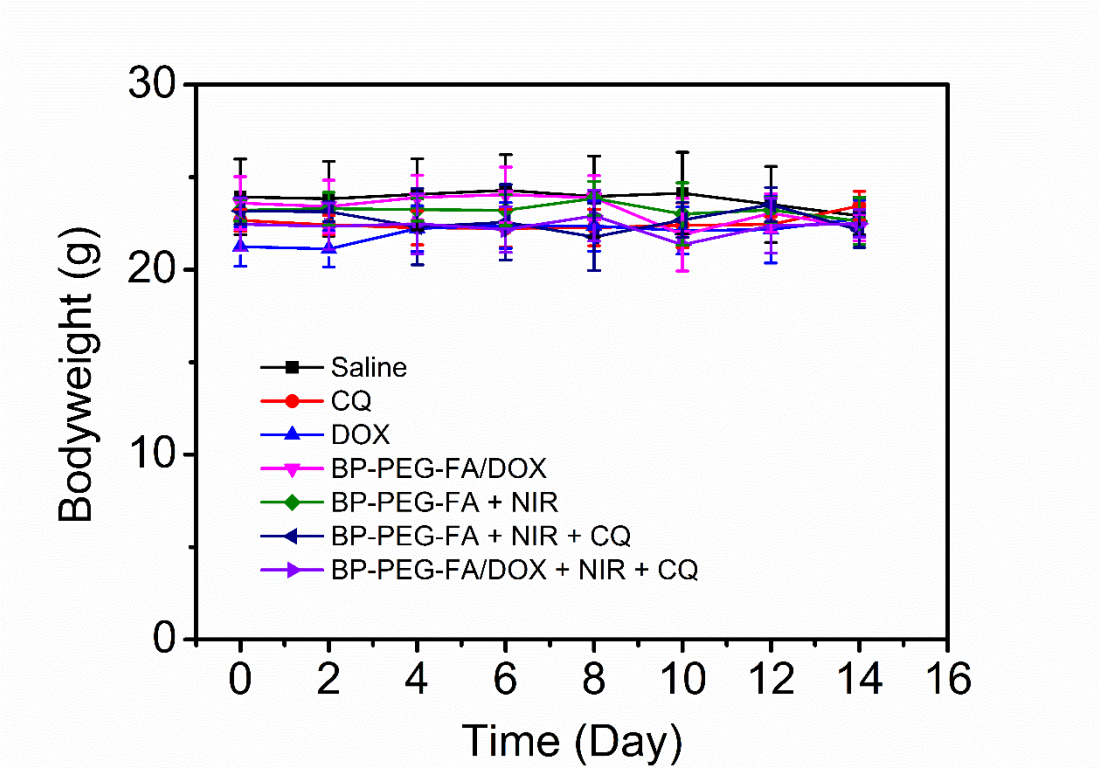

Supporting Figure S32. Body weight of nude mice taken every other day after various treatments with Saline (control), CQ (biological-response control), DOX (chemotherapy control), BP-PEG-FA/DOX NSs(chemotherapy with delivery platform group), BP-PEG-FA NSs followed with 808 nm NIR laser irradiation (PTT group), pre-i.t.-injected CQ together with BP-PEG-FA NSs followed with 808 nm NIR laser irradiation (PTT + biological response-induced therapy group), and pre-i.t.-injected CQ together with BP-PEG-FA/DOX NSs followed with 808 nm NIR laser irradiation (combined triple response group).

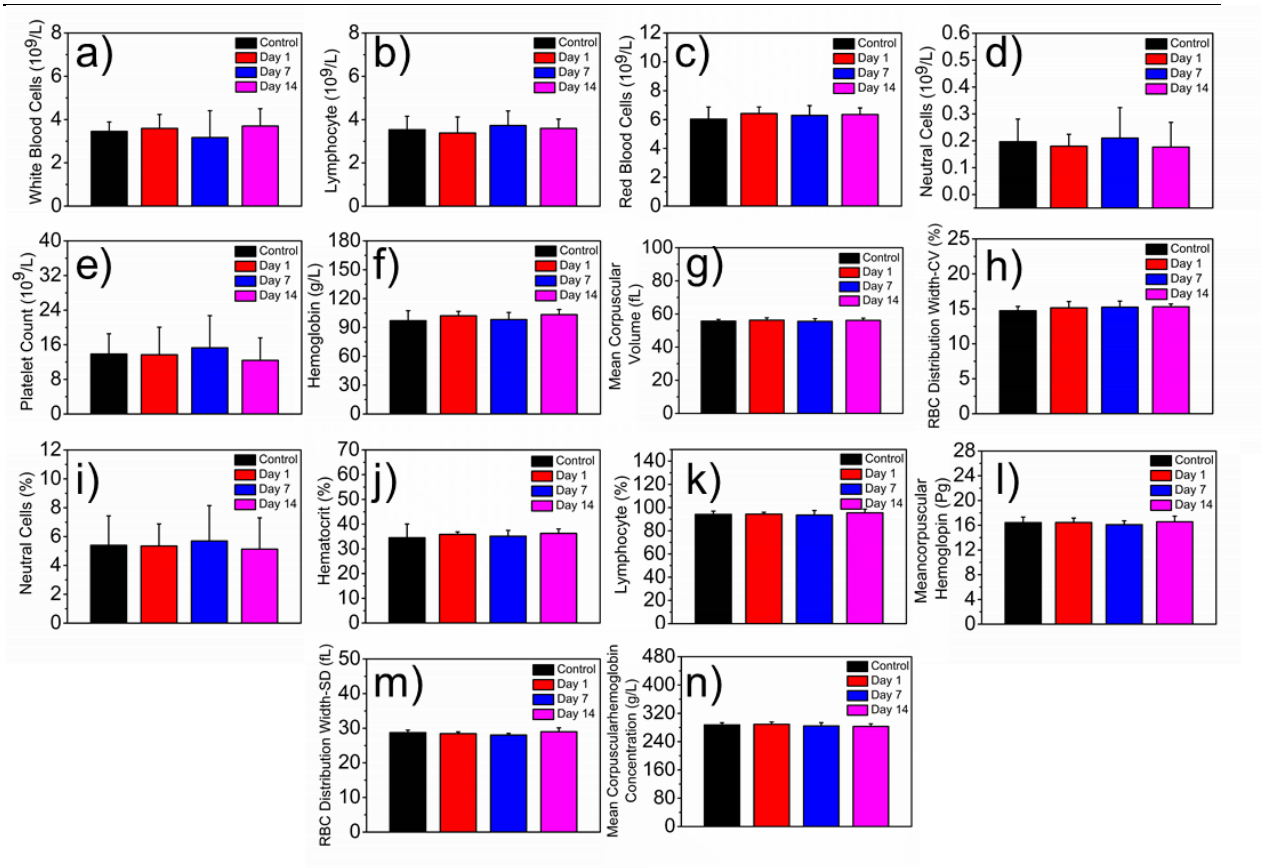

Supporting Figure S33. Blood routine test (BRT) of healthy Balb/c mice *i.v.* injected with BP-PEG NSs at 1, 7 and 14 days for *in vivo* toxicity study. Parameters: a) White Blood Cells (WBC*), b) Lymphocyte (LYM#), c) Red Blood Cells (RBC*), d) Neutral Cells (NEU#), e) Platelet Count (PLT), f) Hemoglobin (Hgb*), g) Mean Corpuscular Volume (MCV), h) RBC Distribution Width-CV (RWD-CV), i) Neutral Cells Percentage (NEU%), j) Hematocrit (HCT), k) Lymphocyte Percentage (LYM%), l) Mean Corpuscular Hemoglopin (MCH), m) RBC Distribution Width-SD (RDW-SD), n) Mean Corpuscular Hemoglobin Concentration (MCHC). The blood of untreated healthy Balb/c mice were used as control.

Reference

[1] H. Wang, X. Yang, W. Shao, S. Chen, J. Xie, X. Zhang, J. Wang, Y. Xie, J Am Chem Soc 2015, 137, 11376.
[2] Z. Sun, H. Xie, S. Tang, X.-F. Yu, Z. Guo, J. Shao, H. Zhang, H. Huang, H. Wang, P. K. Chu, Angewandte Chemie 2015, 127, 11688.

[3] C. Sun, L. Wen, J. Zeng, Y. Wang, Q. Sun, L. Deng, C. Zhao, Z. Li, Biomaterials 2016, 91, 81.
[4] J. T. Robinson, S. M. Tabakman, Y. Liang, H. Wang, H. S. Casalongue, D. Vinh, H. Dai, J Am Chem Soc 2011, 133, 6825.
[5] L. Cheng, J. Liu, X. Gu, H. Gong, X. Shi, T. Liu, C. Wang, X. Wang, G. Liu, H. Xing, W. Bu, B. Sun, Z. Liu, Advanced Materials 2014, 26, 1886.
[6] D. K. Roper, W. Ahn, M. Hoepfner, J Phys Chem C Nanomater Interfaces 2007, 111, 3636.
[7] B. Wang, J. H. Wang, Q. Liu, H. Huang, M. Chen, K. Li, C. Li, X. F. Yu, P. K. Chu, Biomaterials 2014, 35, 1954.
[8] Y. Yang, H. Wu, B. Shi, L. Guo, Y. Zhang, X. An, H. Zhang, S. Yang, Particle & Particle Systems Characterization 2015, 32, 668.
[9] C. M. Hessel, V. P. Pattani, M. Rasch, M. G. Panthani, B. Koo, J. W. Tunnell, B. A. Korgel, Nano Lett 2011, 11, 2560.